



Contents lists available at ScienceDirect

# Journal of Quantitative Spectroscopy & Radiative Transfer

journal homepage: [www.elsevier.com/locate/jqsrt](http://www.elsevier.com/locate/jqsrt)



## High resolution ro-vibrational analysis of interacting bands $\nu_4$ , $\nu_7$ , $\nu_{10}$ , and $\nu_{12}$ of $^{13}\text{C}_2\text{H}_4$



O.N. Ulenikov <sup>a,\*</sup>, O.V. Gromova <sup>a</sup>, E.S. Bekhtereva <sup>a</sup>, C. Maul <sup>b</sup>, S. Bauerecker <sup>b</sup>, M.G. Gabona <sup>c</sup>, T.L. Tan <sup>c</sup>

<sup>a</sup> Institute of Physics and Technology, National Research Tomsk Polytechnic University, Tomsk 634050, Russia

<sup>b</sup> Institut für Physikalische und Theoretische Chemie, Technische Universität Braunschweig, D-38106 Braunschweig, Germany

<sup>c</sup> Natural Sciences and Science Education, National Institute of Education, Nanyang Technological University, 1 Nanyang Walk, Singapore 637616, Singapore

### ARTICLE INFO

#### Article history:

Received 25 August 2014

Received in revised form

26 September 2014

Accepted 30 September 2014

Available online 13 October 2014

#### Keywords:

Ethylene  $^{13}\text{C}_2\text{H}_4$

High-resolution spectra

Spectroscopic parameters

Resonance interactions

### ABSTRACT

High accurate,  $\sim 1 \times 10^{-4} \text{ cm}^{-1}$ , ro-vibrational spectra of the  $^{13}\text{C}_2\text{H}_4$  molecule in the region of  $600$ – $1600 \text{ cm}^{-1}$  were recorded with Bruker IFS 120/125 HR Fourier transform interferometers and analyzed in the Hamiltonian model which takes into account Coriolis resonance interactions between all four bands. More than  $660$ ,  $3870$ ,  $2420$ , and  $2550$  transitions belonging to the  $\nu_4$ ,  $\nu_7$ ,  $\nu_{10}$ , and  $\nu_{12}$  bands were assigned in the experimental spectrum with the maximum values of quantum numbers  $J^{\max.}/K_a^{\max.}$ , equal to  $38/10$ ,  $43/21$ ,  $33/16$  and  $52/18$ , respectively. To make the ro-vibrational analysis physically more suitable, the initial values of the rotational and centrifugal distortion parameters of the studied bands were theoretically estimated by the use of isotopic relations. On that basis, a set of  $55$  vibrational, rotational, centrifugal distortion, and resonance interaction parameters was obtained from the fit. They reproduce values of  $2934$  initial “experimental” ro-vibrational energy levels obtained from nonsaturated unblended lines (more than  $9500$  assigned transitions of the  $\nu_4$ ,  $\nu_7$ ,  $\nu_{10}$ , and  $\nu_{12}$  bands) with the  $rms$  error  $d_{rms} = 0.00014 \text{ cm}^{-1}$ . Ground state parameters of the  $^{13}\text{C}_2\text{H}_4$  molecule were improved as well.

© 2014 Elsevier Ltd. All rights reserved.

### 1. Introduction

Ethylene acts as a hormone in plants and its role in plant biochemistry, physiology, mammal metabolism, and ecology is the subject of extensive research. Ethylene is a naturally occurring compound in ambient air that affects atmospheric chemistry and the global climate. As the result of reaction with the hydroxyl (OH) radical, ethylene plays a significant role in tropospheric chemistry [1], and

ozone generation. This contribution to atmospheric chemistry makes ethylene a climate-relevant trace gas and its air concentration, sources and sinks are of interest to atmospheric science. Ethylene is one of the most relevant substances of study in astrophysics (see, e.g., Refs. [2,3] and has been detected as a trace component of the atmospheres of the outer planets Jupiter, Saturn, Neptune, [4–7], and the satellite Titan, [8–13]. Ethylene has also been observed in circumstellar clouds IRC10216 [2] and CRL618 [3]. Furthermore, ethylene is important as a prototype example in the development of our understanding of relating spectra, dynamics, and potential hypersurfaces of many organic molecules. Therefore, for many years, the

\* Corresponding author.

E-mail address: [Ulenikov@mail.ru](mailto:Ulenikov@mail.ru) (O.N. Ulenikov).

ethylene molecule has been a subject of both extensive experimental (see, e.g. reviews in Refs. [14,15]), and theoretical (see, e.g., Refs. [16,17] and references cited therein) studies (see also recent papers, Refs. [18–20] and information from databases [21,22]).

In the present paper we continue our previous studies of the high resolution ro-vibrational spectra of ethylene and its different isotopic species (for the  $D_{2h}$ -symmetry species see, e.g., Refs. [23–29]). In the present study our attention is focused on the  $^{13}\text{C}_2\text{H}_4$  isotopologue of ethylene. The  $^{13}\text{C}_2\text{H}_4$  spectra were analyzed before only in a few studies, Refs. [23,24,28,30]. In Ref. [30] middle resolution spectra of  $^{13}\text{C}_2\text{H}_4$  were assigned and analyzed. High resolution FTIR spectra in the range of the bands  $\nu_{11}$  and  $\nu_{12}$  were discussed in Refs. [23,24], respectively. Rotational structure of the last band,  $\nu_{12}$ , as well as of the ground vibrational state were studied in the recent paper, Ref. [28].

In the present study we discuss the four lowest interacting vibrational bands,  $\nu_4$ ,  $\nu_7$ ,  $\nu_{10}$ , and  $\nu_{12}$ . The  $\nu_7$  band is the strongest one. The  $\nu_{12}$  band is weaker, and the band  $\nu_{10}$  is considerably weaker than the  $\nu_7$  one. The  $\nu_4$  band is infrared inactive due to the symmetry of the  $^{13}\text{C}_2\text{H}_4$  molecule and its lines only appear in the spectrum because of strong resonance interactions between the ( $\nu_4 = 1$ ) vibrational state, on the one hand, and ( $\nu_7 = 1$ ) and ( $\nu_{10} = 1$ ), on the other hand. In the present study, following the strategy of Ref. [29], we also take into account the presence of resonance interactions between the three mentioned vibrational states and the state ( $\nu_{12} = 1$ ). If one further considers that the value of the ratio  $(M(^{13}\text{C}) - M(^{12}\text{C})) / M(^{13}\text{C})$  is small enough, one can expect that the values of spectroscopic parameters of the  $^{13}\text{C}_2\text{H}_4$  isotopic species will be close to the values of corresponding parameters of the  $^{12}\text{C}_2\text{H}_4$  molecule (see, e.g., Refs. [31–34]).

The structure of the present paper is as following. **Section 2** describes the experimental conditions of the recorded spectra. Description of the experimental spectra and results of assignment of transitions are given in **Section 3**. **Section 4** presents briefly the Hamiltonian model which was used for fitting the experimental line positions. In **Section 5** we present briefly the main

statements of the Isotopic Substitution Theory which were used as the basis for theoretical estimation of initial values of the most important spectroscopic parameters of the  $^{13}\text{C}_2\text{H}_4$  species from the values of corresponding parameters of the mother  $^{12}\text{C}_2\text{H}_4$  molecule. The problems of re-analysis of the ground vibrational state and determination of spectroscopic parameters of the polyad ( $\nu_4 = 1$ )/( $\nu_7 = 1$ )/( $\nu_{10} = 1$ )/( $\nu_{12} = 1$ ) are considered in **Sections 6** and **7**.

## 2. Experimental details

The experimental spectra in the region of 600–1600  $\text{cm}^{-1}$  were recorded with Bruker IFS-125 HR and IFS-120 HR Fourier transform infrared spectrometers in the Infrared Laboratories of Nanyang Technological University and of Technische Universität Braunschweig, respectively. Globar sources, KBr beamsplitters, mercury-cadmium-telluride semiconductor detectors and the sample, 1,2- $^{13}\text{C}_2$  ethylene with a chemical purity of better than 99% purchased from Cambridge Isotope Laboratories, have been used at both places.

The Bruker IFS 125HR Michelson Fourier transform spectrophotometer in the National Institute of Education, Nanyang Technological University, Singapore, was used to record the spectrum of  $^{13}\text{C}_2\text{H}_4$  in the 600–1600  $\text{cm}^{-1}$  region with an unapodized resolution of 0.0063  $\text{cm}^{-1}$ . The spectra were recorded at various vapor pressures ranging from 70.7 to 1460 Pa and pressures were measured using a capacitance pressure gauge. The linewidth (FWHM) in the spectrum was observed to be about 0.0065  $\text{cm}^{-1}$ . For all the spectral measurements at the ambient temperature of about 295 K, we used a multiple-pass absorption cell with 4 passes of 20 cm for each pass to 0.80 m of total absorption path length. It is reasonable to estimate the absolute accuracy of the measured  $^{13}\text{C}_2\text{H}_4$  lines to be better than approximately  $2 \times 10^{-4} \text{ cm}^{-1}$  in the present spectra, after accounting for small systematic errors in the experiments.

In the Braunschweig laboratory four spectra in the 1100–1600  $\text{cm}^{-1}$  region have been recorded in a heatable

**Table 1**

Experimental setup for the regions 600–1600  $\text{cm}^{-1}$  of the infrared spectrum of  $^{13}\text{C}_2\text{H}_4$ .

Spectr.	Region ( $\text{cm}^{-1}$ )	Institute	Resolution ( $\text{cm}^{-1}$ )	Measuring time (h)	No. of scans	Source	Detector	Beam-splitter	Opt. path-length (m)	Aperture (mm)	Temp. (°C)	Pressure (Pa)	Calibr. gas
I	600–1200	Nanyang	0.0063	7.0	420	Globar	MCT	KBr	0.80	1.3	22 ± 0.5	70.7	CO <sub>2</sub>
II	600–1200	Nanyang	0.0063	10.7	640	Globar	MCT	KBr	0.80	1.3	22 ± 0.5	1460	CO <sub>2</sub>
III	1100–1600	Braunschw.	0.0025	9.8	234	Globar	MCT	KBr	16	1.3	23 ± 0.5	17	H <sub>2</sub> O, NO <sub>2</sub>
IV	1100–1600	Braunschw.	0.0025	8.6	204	Globar	MCT	KBr	16	1.3	23 ± 0.5	36	H <sub>2</sub> O, NO <sub>2</sub>
V	1100–1600	Braunschw.	0.0025	16.9	400	Globar	MCT	KBr	24	1.3	23 ± 0.5	150	H <sub>2</sub> O, NO <sub>2</sub>
VI	1100–1600	Braunschw.	0.0025	4.6	110	Globar	MCT	KBr	24	1.3	80 ± 3	180	H <sub>2</sub> O, NO <sub>2</sub>
VII	600–1600	Nanyang	0.0063	17.9	1070	Globar	MCT	KBr	0.80	1.3	22 ± 0.5	230	CO <sub>2</sub>

stainless steel White cell with a base length of 1 m and a maximum path-length of up to 50 m (100 m at laser application). While the resolution of  $0.0025 \text{ cm}^{-1}$  was constant for all spectra, measuring time (4.6–16.9 h), number of scans (110–400), optical path-length (16 and 24 m) and sample gas pressure (17–180 Pa) has been varied to get optimum spectral quality for spectral lines as well with stronger and lower line intensities. The sample temperature was  $296 \pm 0.5 \text{ K}$  except for one spectrum which was recorded at 353 K in order to increase the line intensities for the higher J values at the outer regions of the ro-vibrational band wings. For details see Table 1. The line positions were calculated with the optimized center of gravity method discussed in Ref. [35]. The final spectral resolution was mainly limited by Doppler broadening and resulted in  $0.0032 \text{ cm}^{-1}$  at  $1100 \text{ cm}^{-1}$ , 296 K (minimum), and  $0.0044 \text{ cm}^{-1}$  at  $1600 \text{ cm}^{-1}$ , 353 K (maximum). The contribution of the pressure broadening to the final spectral resolution is marginal for sample pressures up to a few hundred Pa. The wavenumber accuracy of non-blended, unsaturated and not too weak lines can be estimated to be better than  $10^{-4} \text{ cm}^{-1}$  in the presented spectral region.

### 3. Description of the spectra and assignment of transitions

The survey spectra I and II in the region of  $600\text{--}1200 \text{ cm}^{-1}$ , and III and IV in the region of  $1300\text{--}1600 \text{ cm}^{-1}$ , where the  $\nu_7$ ,  $\nu_{10}$ , and  $\nu_{12}$  bands of the  $^{13}\text{C}_2\text{H}_4$  molecule are located, are shown in Figs. 1, 2 and 3, respectively. The band  $\nu_7$  is the strongest absorption band in the discussed region (see Fig. 4). As can be seen in

Fig. 4, the  $\nu_{12}$  band is weaker than the  $\nu_7$  one, and the  $\nu_7$  band is considerably weaker in comparison with the  $\nu_{10}$  band (one can get an impression about relative intensities of the  $\nu_7$  and  $\nu_{10}$  bands from Figs. 1, 2, and 4; the P-branch of the  $\nu_{10}$  band is clearly pronounced in the two last figures). The  $\nu_4$  band is forbidden in absorption by the symmetry of the molecule. As a consequence, its transitions appear in the experimental spectrum only because of the intensity transfer from the ( $\nu_7 = 1$ ) band to the ( $\nu_4 = 1$ ) band caused by the strong c-type Coriolis interactions between the state ( $\nu_4 = 1$ ) and ( $\nu_7 = 1$ ). For that reason, transitions belonging to the  $\nu_4$  band are very weak as a rule, in comparison with transitions of the  $\nu_7$  band, and the  $\nu_4$  band is not pronounced in the overview spectra. However, in the high resolution spectrum (see Fig. 5 as an illustration) sets of transitions of the  $\nu_4$  band (they are marked by dark circles) can be clearly seen. Lines of the band  $\nu_7$  and one line of the band  $\nu_{10}$  are also shown (they are marked by dark and empty triangles, respectively). Experimental conditions of Fig. 5 correspond to the spectrum I.

The  $^{13}\text{C}_2\text{H}_4$  molecule is an asymmetric top with the value of the asymmetry parameter  $\kappa \approx (2B - A - C)/(A - C) = -0.973$  and with the symmetry isomorphic to the  $D_{2h}$  point symmetry group (see Fig. 6). Three types of absorption bands are allowed in absorption from the ground vibrational state by the symmetry properties of a molecule:

- (1) the  $B_{1u} \leftarrow A_g$  bands are the c-type ones, and the selection rules for them are:  $\Delta J = 0, \pm 1$  and  $\Delta K_a = \text{odd}$ ,  $\Delta K_c = \text{even}$ ;
- (2) the  $B_{2u} \leftarrow A_g$  bands are the b-type ones, and the selection rules for them are:  $\Delta J = 0, \pm 1$  and  $\Delta K_a = \text{odd}$ ,  $\Delta K_c = \text{odd}$ ;

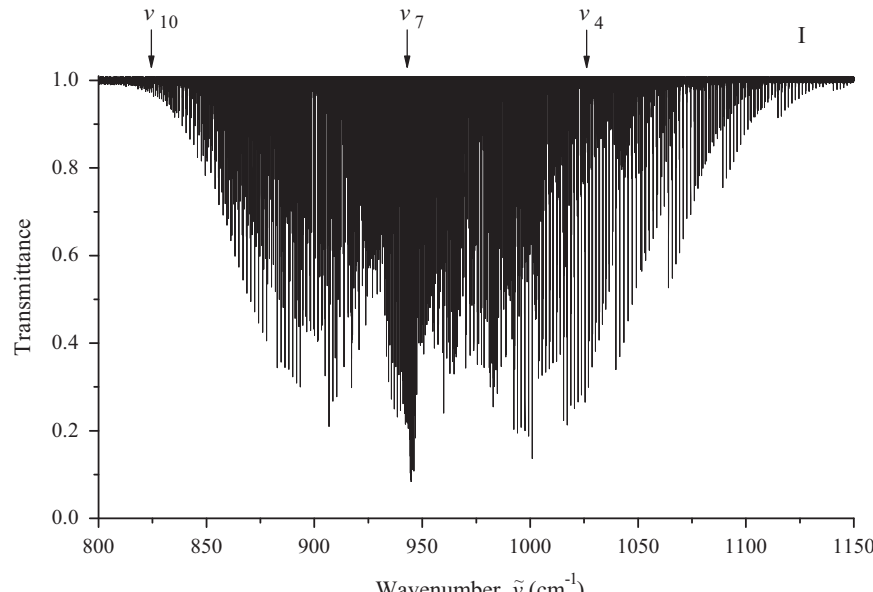


**Fig. 1.** Survey spectrum I of  $^{13}\text{C}_2\text{H}_4$  in the region of the  $\nu_7$ ,  $\nu_{10}$ , and  $\nu_4$  bands. The  $\nu_{10}$  band is hardly visible in the spectrum. Experimental conditions: sample pressure is 70.7 Pa, absorption path length is 0.80 m; room temperature, 295 K; number of scans is 420.

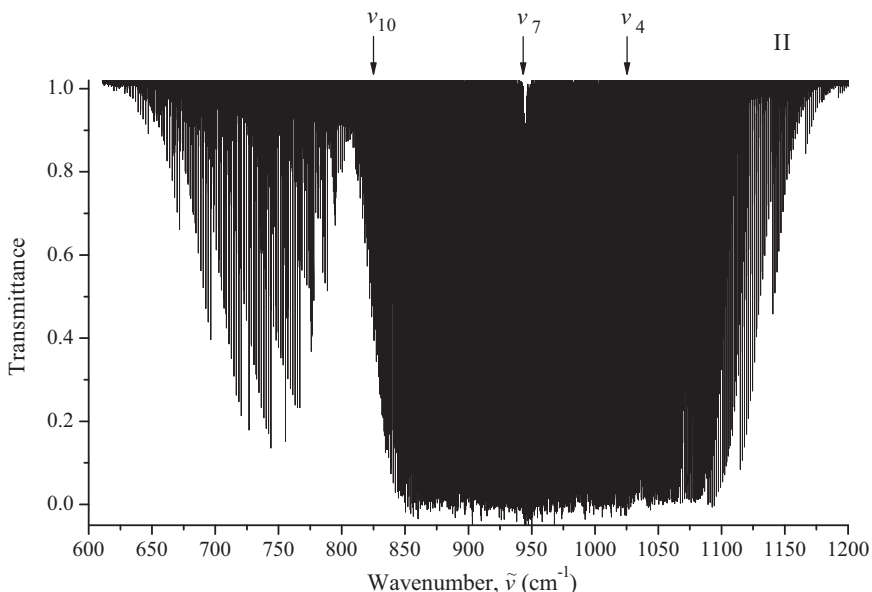


**Fig. 2.** Survey spectrum II of  $^{13}\text{C}_2\text{H}_4$  in the region of the  $\nu_7$ ,  $\nu_{10}$ , and  $\nu_4$  bands. The  $\nu_{10}$  band is clearly pronounced in the left side of the figure. Experimental conditions: sample pressure is 1460 Pa, absorption path length is 0.80 m; room temperature, 295 K; number of scans is 640.

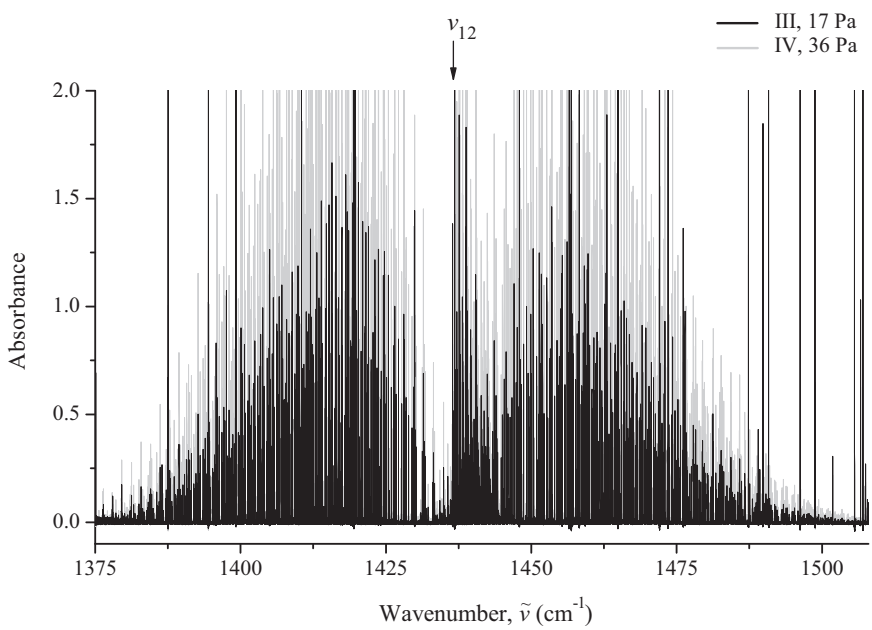


**Fig. 3.** Survey spectra III ("black") and IV ("grey") of  $^{13}\text{C}_2\text{H}_4$  in the region of the  $\nu_{12}$  band. For experimental conditions see Table 1.

(3) the  $B_{3u} \leftarrow A_g$  bands are the a-type ones, and the selection rules for them are:  $\Delta J = 0, \pm 1$  and  $\Delta K_a = \text{even}$ ,  $\Delta K_c = \text{odd}$ .

For this reason the  $\nu_7$ ,  $\nu_{10}$ ,  $\nu_{12}$ , and  $\nu_4$  bands can be identified as the c-type, b-type, a-type, and forbidden one, respectively.

Assignment of transitions was made with the Ground State Combination Differences (GSCD) method (see, for

details, Section 6). As the result of assignment, more than 660, 3870, 2420, and 2550 transitions (in general, more than 9500 transitions from which the 2934 ro-vibrational energy levels for four upper vibrational states were obtained) with the maximum values of upper quantum numbers,  $J^{\max}/K_a^{\max}$ , equal to 38/10, 43/21, 33/16 and 52/18 have been assigned to the  $\nu_4$ ,  $\nu_7$ ,  $\nu_{10}$ , and  $\nu_{12}$  bands, respectively (for more details, see statistical information in Table 2). Previously, only the  $\nu_{12}$  band was analyzed, and

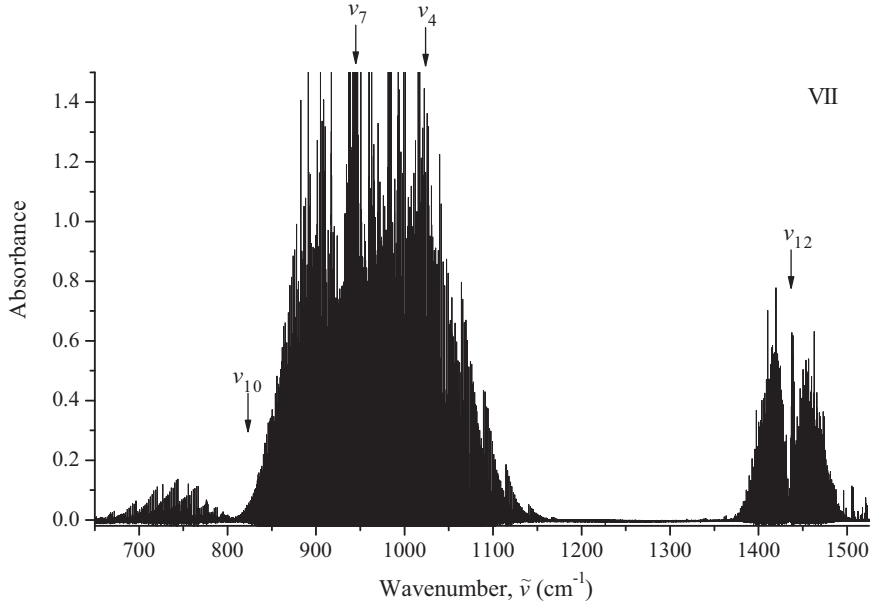


**Fig. 4.** Survey spectrum of  $^{13}\text{C}_2\text{H}_4$  in the whole region of 600–1600  $\text{cm}^{-1}$ . Relative strengths of separate bands are clearly pronounced. Experimental conditions: sample pressure is 230 Pa, absorption path length is 0.80 m; room temperature, 295 K; number of scans is 1070.

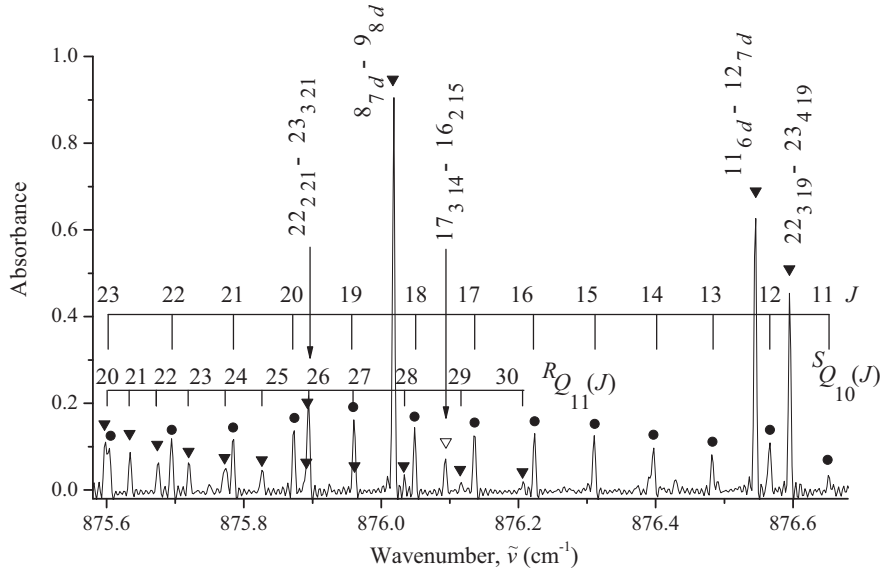


**Fig. 5.** A small part of the high resolution spectrum of the  $^{13}\text{C}_2\text{H}_4$  molecule in the region of  $P$ -branch of the  $\nu_7$  band. Experimental conditions correspond to the “weak” spectrum I: sample pressure, 70.7 Torr; absorption path length, 0.80 m; room temperature, 295 K; 420 scans. Transitions assigned to the  $\nu_7$  band and to the single line of the  $\nu_{10}$  band are marked by the dark and empty triangles, respectively. The clearly pronounced set of  $Q$ -type transitions of the “forbidden”  $\nu_4$  band can be seen also. These transitions are marked by dark circles.

transitions with  $J^{\max} = 41$  and  $K_a^{\max} = 16$  were assigned. The three other bands are analyzed in the present study for the first time.

#### 4. Hamiltonian model

As the analysis shows, the studied bands of  $^{13}\text{C}_2\text{H}_4$  strongly interact with each other. Therefore, we used in the further analysis the effective Hamiltonian model of an

asymmetric top molecule which takes into account the presence of interaction operators of different symmetry (see, e.g., Refs. [36–48]):

$$H^{\text{vib.-rot.}} = \sum_{\nu, \tilde{\nu}} |\nu\rangle \langle \tilde{\nu}| H^{\nu\tilde{\nu}}, \quad (1)$$

where the summation is taken from 1 to 4 for both  $\nu$  and  $\tilde{\nu}$ , which represent the four vibrational states mentioned above:  $A_u$ -symmetry:  $|1\rangle = (\nu_4 = 1)$ ,  $B_{2u}$ -symmetry:  $|2\rangle =$

$(v_{10} = 1)$ ,  $B_{3u}$ -symmetry:  $|3\rangle = (v_{12} = 1)$ , and  $B_{1u}$ -symmetry:  $|4\rangle = (v_7 = 1)$ .

Any of the diagonal blocks  $H^{vv}$ , Eq. (2), describes the unperturbed rotational structure of the vibrational state  $|v\rangle$  and has a form of the reduced effective Hamiltonian in the  $A$ -reduction and  $I'$  representation (see, e.g., Refs. [49–52]):

$$\begin{aligned} H_{vv} = E^v + \left[ A^v - \frac{1}{2}(B^v + C^v) \right] J_z^2 + \frac{1}{2}(B^v + C^v) J^2 + \frac{1}{2}(B^v - C^v) J_{xy}^2 \\ - \Delta_{Kz}^v J_z^4 - \Delta_{JK}^v J_z^2 J^2 - \Delta_J^v J^4 - \delta_K^v [J_z^2, J_{xy}^2]_+ - 2\delta_J^v J_z^2 J_{xy}^2 \\ + H_{KJz}^v + H_{KJz}^v J_z^2 + H_{JKz}^v J_z^4 + H_{vJ}^v \\ + [J_{xy}^2, h_{KJz}^v J_z^4 + h_{JKz}^v J_z^2 + h_J^v J^4]_+ \\ + L_{KJz}^v J_z^8 + L_{KKJz}^v J_z^6 + L_{JKJz}^v J_z^4 \\ + L_{KJz}^v J_z^6 + L_J^v J^8 + [J_{xy}^2, l_{KJz}^v J_z^6 + l_{KJz}^v J_z^4 + l_{JKz}^v J_z^2 + l_J^v J^6]_+ + \dots, \end{aligned} \quad (2)$$

where  $J_{xy}^2 = J_x^2 - J_y^2$ ;  $[..., ...]_+$  denotes the anticommutator;  $A^v$ ,  $B^v$ , and  $C^v$  are the effective rotational constants connected with the vibrational state  $v$ , and other parameters are the different order centrifugal distortion coefficients. Nondiagonal blocks  $H^{v\tilde{v}}$  ( $v \neq \tilde{v}$ ) describe four different kinds of resonance interactions between vibrational states of the  $u$ -type symmetries:  $A_u$ ,  $B_{1u}$ ,  $B_{2u}$ , and  $B_{3u}$ . In our case, all four considered vibrational states have different symmetry. For that reason, only Coriolis-type interactions should be present in the Hamiltonian, Eq. (1), by the three different operators the parts of which (proportional to  $iJ_x$ ,  $iJ_y$ , and  $iJ_z$ ) are transformed in accordance with the irreducible representations  $B_{2g}$ ,  $B_{1g}$ , and  $B_{3g}$  of the  $D_{2h}$  group. First, if  $(|v\rangle\Gamma_u) \otimes (|\tilde{v}\rangle\tilde{\Gamma}_u) = B_{1g}$ , then the interaction

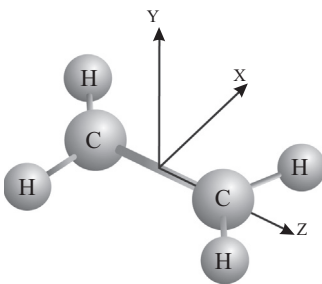


**Fig. 6.** Axes definitions used in the present work for the ethylene,  $^{13}\text{C}_2\text{H}_4$ , molecule. The symbols refer to the Cartesian axis definitions of the  $I'$  representation of Watson's  $A$ -reduced effective Hamiltonian.

operator can be written as

$$H_{v\tilde{v}} = iJ_y H_{vv}^{(1)} + H_{vv}^{(1)} iJ_y + [J_x, J_z]_+ H_{vv}^{(2)} + H_{vv}^{(2)} [J_x, J_z]_+ + \dots \quad (3)$$

Second, if  $(|v\rangle\Gamma_u) \otimes (|\tilde{v}\rangle\tilde{\Gamma}_u) = B_{2g}$ , the corresponding Coriolis-interaction operator has the form

$$H_{v\tilde{v}} = iJ_x H_{vv}^{(1)} + H_{vv}^{(1)} iJ_x + [J_y, J_z]_+ H_{vv}^{(2)} + H_{vv}^{(2)} [J_y, J_z]_+ + \dots \quad (4)$$

In the third case, if  $(|v\rangle\Gamma_u) \otimes (|\tilde{v}\rangle\tilde{\Gamma}_u) = B_{3g}$ , the Coriolis-interaction operator is

$$H_{v\tilde{v}} = iJ_z H_{vv}^{(1)} + [J_x, J_y]_+ H_{vv}^{(2)} + H_{vv}^{(2)} [J_x, J_y]_+ + \dots \quad (5)$$

The  $H_{vv}^{(i)}$  ( $i = 1, 2$ ) in Eqs. (3)–(5) are also operators, and they can be written in a general form as

$$\begin{aligned} H_{vv}^{(i)} = \frac{1}{2} v\tilde{v} C^i + v\tilde{v} C_{KJz}^i J_z^2 + \frac{1}{2} v\tilde{v} C_J^i J^2 + v\tilde{v} C_{KKJz}^i J_z^4 + v\tilde{v} C_{KJz}^i J_z^2 \\ + \frac{1}{2} v\tilde{v} C_{JJz}^i J_z^4 + \dots \end{aligned} \quad (6)$$

The axis notation of the  $\text{C}_2\text{H}_4$  molecule is shown in Fig. 6.

## 5. Isotopic relations for substitution $^{13}\text{C}_2\text{H}_4 \leftarrow ^{12}\text{C}_2\text{H}_4$

In this section we present briefly some information from the Isotopic Substitution Theory, Refs. [31–34], which allowed us to derive a set of simple isotopic relations which were used then for estimation of initial numerical values of spectroscopic parameters (vibrational, rotational, centrifugal distortion, and resonance interaction parameters) of the polyad  $(v_4 = 1)/(v_7 = 1)/(v_{10} = 1)/(v_{12} = 1)$ .

There are three main sets of formulas in the Isotopic Substitution Theory which can be considered as the basis for the derivation of numerous isotopic relations for different type molecules. They are as follows:

- (1) A set of equations which allow one either to determine all harmonic frequencies,  $\omega'_\nu$ , of any isotopically substituted molecule as functions of the harmonic frequencies,  $\omega_\lambda$ , of a parent molecule and a set of coefficients  $A_{\lambda\mu}$ ; or, oppositely, to determine coefficients  $A_{\lambda\mu}$  as functions of the harmonic frequencies of the parent and the substituted molecule:

$$\sum_\lambda A_{\lambda\mu} \omega_\lambda^2 \alpha_{\nu\lambda} = \alpha_{\nu\lambda} \omega'_\nu^2. \quad (7)$$

The  $\alpha_{\nu\lambda}$  are additional coefficients which are also determined from solving the set of equations (7).

**Table 2**

Statistical information for the  $\nu_4$ ,  $\nu_7$ ,  $\nu_{10}$ , and  $\nu_{12}$  bands of the  $^{13}\text{C}_2\text{H}_4$  molecule.

Band 1	Center ( $\text{cm}^{-1}$ ) 2	$J^{\max}$ 3	$K_a^{\max}$ 4	$N_t^a$ 5	$N_l^b$ 6	$rms$ 7	$m_1^c$ 8	$m_2^c$ 9	$m_3^c$ 10
$\nu_4$	1025.80428	38	10	660	228	0.00015	50.8	26.8	22.4
$\nu_7$	943.76251	43	21	3870	1049	0.00013	70.3	21.2	8.5
$\nu_{10}$	824.91511	33	16	2420	593	0.00016	62.4	21.6	16.0
$\nu_{12}$	1436.65101	52	18	2550	1064	0.00014	67.9	18.0	14.1

<sup>a</sup>  $N_t$  is the number of transitions.

<sup>b</sup>  $N_l$  is the number of upper levels.

<sup>c</sup> Here  $m_i = n_i/N \times 100\%$  ( $i = 1, 2, 3$ );  $n_1$ ,  $n_2$ , and  $n_3$  are the numbers of levels (transitions) for which the differences  $\delta = E^{\text{exp.}} - E^{\text{calc.}}$  ( $\delta = \nu^{\text{exp.}} - \nu^{\text{calc.}}$ ) satisfy the conditions  $\delta \leq 1 \times 10^{-4} \text{ cm}^{-1}$ ,  $1 \times 10^{-4} \text{ cm}^{-1} < \delta \leq 2 \times 10^{-4} \text{ cm}^{-1}$ , and  $\delta > 2 \times 10^{-4} \text{ cm}^{-1}$ .

**Table 3**

Values of the center shifts of the bands  $\nu_4$ ,  $\nu_7$ ,  $\nu_{10}$ , and  $\nu_{12}$  (in  $\text{cm}^{-1}$ ).

Band shift	Predict.	Exp.
1	2	3
$\Delta\nu_4$	0.00	+0.21
$\Delta\nu_7$	- 5.12	- 5.01
$\Delta\nu_{10}$	- 0.98	- 1.01
$\Delta\nu_{12}$	- 5.96	- 5.79

(2) The second set of the above mentioned formulas has the following form ( $m_N$  and  $m'_N$  are the masses of atoms before and after isotopic substitution):

$$A_{\lambda\mu} = \delta_{\lambda\mu} - \sum_{Na} \frac{(m'_N - m_N)}{m'_N} l_{Na\lambda} l_{Na\mu}, \quad (8)$$

and they determine the  $A_{\lambda\mu}$  coefficients via the so-called transformation coefficients,  $l_{Na\lambda}$ , of a parent isotopomer. Usually these transformation coefficients are known for any parent isotopomer, or can be easily obtained from a set of known equations, (see, e.g., Ref. [53]).

(3) The third type formulas can be written as

$$l'_{N\gamma\lambda} = \sum_{\alpha\mu} K_{\alpha\gamma}^e \left( \frac{m_N}{m'_N} \right)^{1/2} l_{Na\mu} (\alpha^{-1})_{\mu\lambda} \quad (9)$$

and they provide the possibility to calculate transformation coefficients of a substituted isotopomer as functions of characteristics of the parent species. Here  $K_{\alpha\gamma}^e$  is the matrix that provides a rotation of the molecular equilibrium coordinate axes from the parent species to a substituted one (in our present case, the matrix  $K_{\alpha\gamma}^e = \delta_{\alpha\gamma}$ ). In Eqs. (7)–(9),  $\alpha, \gamma = x, y, z$ ;  $\lambda, \mu, \nu$  numerate vibrational modes.

If one solves Eqs. (7)–(9) for the isotopic substitution  $^{13}\text{C}_2\text{H}_4 \leftarrow ^{12}\text{C}_2\text{H}_4$  and takes into account that the values of the anharmonic coefficients  $x_{\lambda\mu}$  are practically unchanged under such a substitution, then it is possible to show that the centers of the bands  $\nu_4$ ,  $\nu_7$ ,  $\nu_{10}$ , and  $\nu_{12}$  are shifted for the isotopic substitution by the values presented in column 2 of Table 3. Column 3 presents corresponding experimental values, which are differences between experimental band centers from Ref. [27] and corresponding band centers from Section 7 of this paper. One can see a good agreement between predicted and experimental values. We believe that this is a good confirmation of the validity both of the above general formulas, and the numerical estimations of the most important (rotational and the main resonance Coriolis interaction) spectroscopic parameters of the  $^{13}\text{C}_2\text{H}_4$  species on the basis of corresponding parameters of the main,  $^{12}\text{C}_2\text{H}_4$ , molecule (the latter parameters have been taken from Ref. [27]).

If one applies the general formulas (7)–(9) to the isotopic substitution  $^{13}\text{C}_2\text{H}_4 \leftarrow ^{12}\text{C}_2\text{H}_4$ , then it is possible to show that the values of all ro-vibrational coefficients  $\alpha_{\lambda}^{\beta}$  are changed only by a few percent. In turn, taking into account that the ro-vibrational coefficients  $\alpha_{\lambda}^{\beta}$  themselves are small values (about 4–6%) in comparison with the values of equilibrium rotational parameters, one can conclude that the change of the values of the effective

**Table 4**

Estimated values of effective rotational parameters,  $A, B, C$ , for some vibrational states of  $^{13}\text{C}_2\text{H}_4$  (in  $\text{cm}^{-1}$ ).

State	A	B	C
1	2	3	4
( $\nu_4 = 1$ )	4.8462	0.9480	0.7934
( $\nu_7 = 1$ )	4.8690	0.9481	0.7945
( $\nu_{10} = 1$ )	4.8735	0.9493	0.7918
( $\nu_{12} = 1$ )	4.8521	0.9531	0.7917

**Table 5**

Estimated values of some effective Coriolis interaction parameters,  $2B_{\beta\zeta\lambda\mu}^{ef}$ , of  $^{13}\text{C}_2\text{H}_4$  (in  $\text{cm}^{-1}$ ).

$\lambda\mu$	Value, $^{13}\text{C}$	Value, $^{12}\text{C}$
1	2	3
4/7	0.00	0.00
4/10	- 1.68	- 1.76868
4/12	- 5.48	- 5.5133766
7/10	- 4.40	- 4.3829518
7/12	- 1.25	- 1.3422097
10/12	0.13	0.143289

rotational parameters is defined only by the change of the values of the equilibrium rotational parameters. The values of the effective rotational parameters of  $^{13}\text{C}_2\text{H}_4$  estimated by that way from the values of the corresponding rotational parameters of the  $^{12}\text{C}_2\text{H}_4$  molecule,

Ref. [27], are presented in Table 4.

Another important set of spectroscopic parameters should be estimated theoretically. These are the main parameters which describe different type Coriolis interactions. Usually such parameters are determined from a fit with only low accuracy. As a consequence, the best way is to estimate such parameters theoretically and then to fix them in the fit procedure. In our case, we again used corresponding resonance Coriolis parameters from Ref. [27] for prediction of the parameter values of the  $^{13}\text{C}_2\text{H}_4$  species. These estimated values (presented in column 2 of Table 5) were then used in the fit procedure as constrained parameters. Column 3 of Table 5 gives, for comparison, initial values of the corresponding parameters of the  $^{12}\text{C}_2\text{H}_4$  molecule from Ref. [27].

## 6. Re-analysis of the ground vibrational state

In the first step of the analysis, the rotational energies of the ground vibrational state from Ref. [28] were used for the assignment of transitions. For the  $\nu_{12}$  band we found that the ground state parameters from Ref. [28] produce highly accurate GSCD even for larger  $J$  quantum numbers than it was in Ref. [28]. On the other hand, it was found also, that for the other three bands,  $\nu_7$ ,  $\nu_{10}$ , and  $\nu_4$ , the quality of GSCD strongly deteriorates with increasing values of both quantum numbers  $J$ , and, especially  $K_a$  (the values of some sets of differences between “experimental” and calculated GSCD increased up to  $0.4 \text{ cm}^{-1}$  already for values  $J \approx 16 - 17$  and/or  $K_a \approx 16 - 17$ , see Fig. 7 for illustration). This can be explained by the fact that the

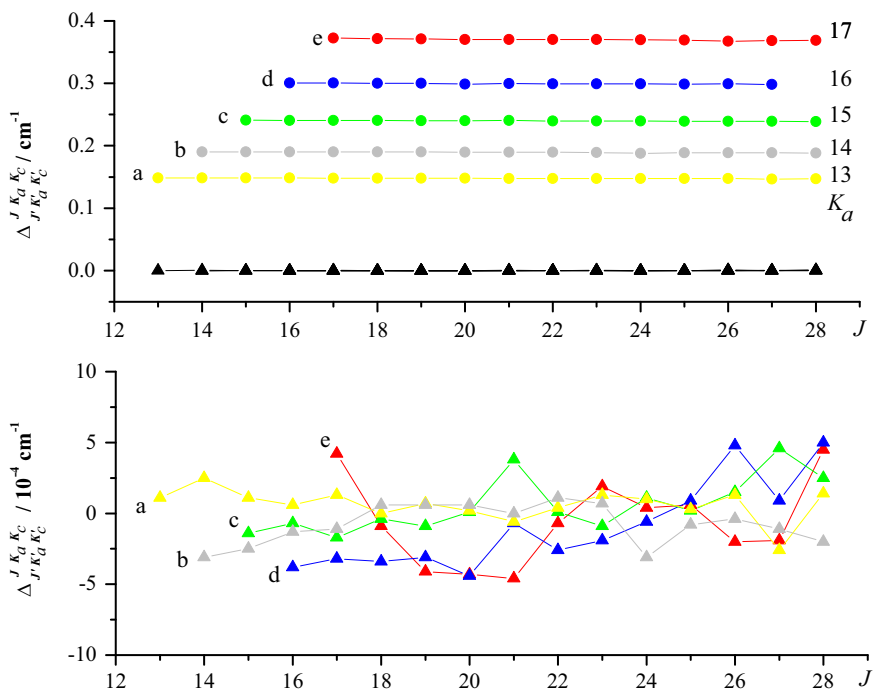


**Fig. 7.** Plots of dependency of differences  $\Delta_{J'K_a'K_c}^{JK_aK_c} = (\text{exp.})\delta_{J'K_a'K_c}^{JK_aK_c} - (\text{calc.})\delta_{J'K_a'K_c}^{JK_aK_c}$  (here  $\delta_{J'K_a'K_c}^{JK_aK_c} = E_{JK_aK_c} - E_{J'K_a'K_c}$ ;  $J' = J + 2$ ,  $K'_a = K_a + 2$ ) between experimental and calculated values of some sets of ground state combination differences on the value of quantum number  $J$ . Curves of different colors (curves a, b, c, d, and e on the top part of the figure) correspond to the values  $K_a$  equal 13, 14, 15, 16, and 17, respectively. These curves have been constructed with the theoretically calculated combination differences,  $(\text{calc.})\delta_{J'K_a'K_c}^{JK_aK_c}$ , obtained on the base of the ground state parameters from Ref. [28] (see also column 4 of Table 6). Curves on the bottom part of the figure correspond to results obtained on the base of our ground state parameters from column 2 of Table 6. For more details, the same results are reproduced on the bottom part of that figure. (For interpretation of the references to color in this figure caption, the reader is referred to the web version of this article.)

**Table 6**

Spectroscopic parameters of the ground vibrational state of the  $^{13}\text{C}_2\text{H}_4$  molecule (in  $\text{cm}^{-1}$ )<sup>a</sup>.

Parameter	$^{13}\text{C}_2\text{H}_4$ , this work 1	$^{12}\text{C}_2\text{H}_4$ , from [27] <sup>b</sup> 2	$^{13}\text{C}_2\text{H}_4$ , from [28] <sup>c</sup> 3	$^{13}\text{C}_2\text{H}_4$ , from [28] <sup>c</sup> 4
$A$	4.864792048(121)	4.86461997815	4.86483	
$B$	0.9506945106(777)	1.00105650691	0.9506899	
$C$	0.7932735014(896)	0.82804595595	0.7932782	
$\Delta_K \times 10^4$	0.8701743(101)	0.86470155	0.94	
$\Delta_{JK} \times 10^4$	0.09815297(367)	0.102336194	0.0987	
$\Delta_J \times 10^4$	0.013386718(333)	0.014701077	0.013352	
$\delta_K \times 10^4$	0.0953733(156)	0.10153495	0.0955	
$\delta_J \times 10^4$	0.002452716(179)	0.0028179017	0.0022424	
$H_K \times 10^8$	0.628947(179)	0.621279		
$H_{JK} \times 10^8$	– 0.0431669(558)	– 0.041497	0.013	
$H_{JK} \times 10^8$	0.0166920(207)	0.018693	0.0079	
$H_J \times 10^8$	0.00029659(102)	0.00023588	0.000067	
$h_K \times 10^8$	0.34059	0.34059		
$h_{JK} \times 10^8$	0.0103566	0.0103566		
$h_J \times 10^8$	0.000125178	0.000125178		
$L_K \times 10^{12}$	– 0.4467	– 0.4467		
$L_{JK} \times 10^{12}$	– 0.004492	– 0.004492		
$L_J \times 10^{12}$	– 0.0000172	– 0.0000172		

<sup>a</sup> Values in parentheses are  $1\sigma$  standard errors.

<sup>b</sup> Reproduced from Ref. [27, Table 5].

<sup>c</sup> Reproduced from the third column of Table 1, Ref. [28].

band  $\nu_{12}$ , which was used in Ref. [28] for determination of GSCD, is an *a*-type band. As a consequence of this, only  $\Delta K_a = 0$  ground state combination differences can be constructed from allowed transitions of that band and the parameters  $B$ ,  $C$ ,  $\Delta_J$ ,  $H_j$ ,  $L_j$ , ..., can be correctly determined from such ground state combination differences. At the same time, the bands  $\nu_7$  and  $\nu_{10}$  are of *c*- and *b*-type, respectively. Consequently not only  $\Delta K_a = 0$ , but also  $\Delta K_a = \pm 2$  combination differences are produced by the allowed transitions. To reproduce values for such combination differences, it is necessary to have correct values of not only the above mentioned  $B$ ,  $C$ ,  $\Delta_J$ ,  $H_j$ ,  $L_j$  parameters, but of the parameters  $A$ ,  $\Delta_{JK}$ ,  $\Delta_K$ , etc., as well. In summary the new analysis of the rotational structure of the ground vibrational states is suitable on the basis of ground state combination differences which should be determined not only from transitions of the  $\nu_{12}$  band, but of the bands  $\nu_7$ ,  $\nu_{10}$ , and  $\nu_4$ , as well.

In our present analysis we were able to construct more than 11,000 GSCD with the values  $J^{\max.} = 50$  ( $\Delta J = 0, \pm 2$ ),  $K_a^{\max.} = 18$  ( $\Delta K_a = 0, \pm 2$ ), and  $\Delta K_c = 0, \pm 2, \pm 4$ . However we did not use all of them in the further fit procedure, but only those which were obtained as mean values of GSCD obtained both from different bands and from different sets of transitions of the same band. As a rule, uncertainties of such mean values were less than  $0.00013\text{ cm}^{-1}$ . Finally, we constructed more than 250 highly accurate mean GSCD values, which were then used in the weighted fit of rotational and centrifugal distortion parameters of the ground vibrational state (the weights have been taken proportional to the values  $(1/\Delta)^2$ , where  $\Delta$  are the experimental uncertainties in the upper energy values). Parameters obtained from the fit are presented in column 2 of Table 6. Values in parenthesis are  $1\sigma$  statistical confidence intervals. Higher order centrifugal distortion parameters which are presented without confidence intervals have been constrained to the values of corresponding parameters of the  $^{12}\text{C}_2\text{H}_4$  molecule (for the convenience of the reader, the latter are reproduced from Ref. [27] in column 3 of Table 6). As expected, the values of the obtained parameters of the  $^{13}\text{C}_2\text{H}_4$  species do not strongly differ from the values of the corresponding parameters of  $^{12}\text{C}_2\text{H}_4$ . Column 4 of Table 6 presents, for comparison, a set of earlier determined parameters from Ref. [28]. The *rms* deviation of the above mentioned 250 GSCD, used in the present fit and calculated with the parameters from Ref. [28], is  $0.103334\text{ cm}^{-1}$ . Calculated with the set of parameters from column 2 of Table 6, that value decreased to  $0.000093\text{ cm}^{-1}$ . The lower part of Fig. 6 also illustrates the quality of the improved set of parameters of the ground vibrational state.

## 7. Ro-vibrational analysis of interacting states ( $\nu_4 = 1$ , $\nu_7 = 1$ , $\nu_{10} = 1$ , and $\nu_{12} = 1$ )

The new ground state parameters obtained in Section 6 were then used for the calculation of ground state rotational energies which, in turn, were used in the re-assignments of transitions in the recorded FTIR spectra of the bands  $\nu_4$ ,  $\nu_7$ ,  $\nu_{10}$ , and  $\nu_{12}$ . The list of more than 9500 finally assigned transitions is presented in the Supplementary Materials. From these transitions we obtained 2934

upper ro-vibrational energies: 228 ( $J^{\max.} = 38$ ,  $K_a^{\max.} = 10$ ), 1049 ( $J^{\max.} = 43$ ,  $K_a^{\max.} = 21$ ), 593 ( $J^{\max.} = 33$ ,  $K_a^{\max.} = 16$ ), and 1064 ( $J^{\max.} = 52$ ,  $K_a^{\max.} = 18$ ) upper energies for the states ( $\nu_4 = 1$ ), ( $\nu_7 = 1$ ), ( $\nu_{10} = 1$ ), and ( $\nu_{12} = 1$ ), respectively (in this case, only nonsaturated unblended lines were used for the determination of upper energy values). These were then used as input data in a weighted least square fit with the aim to determine rotational, centrifugal distortion, and resonance interaction parameters for the studied vibrational states. As an illustration, a small part of the upper energies for the vibrational states ( $\nu_7 = 1$ ), ( $\nu_{10} = 1$ ), and ( $\nu_{12} = 1$ ) are shown in Table 7 together with their experimental uncertainties,  $\Delta$  and the values of  $\delta = E^{\exp.} - E^{\text{calc.}}$  ( $E^{\exp.}$  and  $E^{\text{calc.}}$  are the values of upper energies obtained from experimental line positions and from calculations on the basis of parameters obtained from the fit). The upper energies of the ( $\nu_4 = 1$ ,  $A_u$ ) state are listed in Table 8.

The Hamiltonian discussed in Section 4 was used as the basis for the fit procedure. In this case, the initial values of the vibrational, rotational and main Coriolis interaction parameters were taken from numerical estimation on the basis of isotopic relation (see Table 4 and columns 2 of Tables 3 and 5). The initial values of centrifugal distortion parameters for all four upper vibrational states have been taken from the ground vibrational state (Table 6). The values of resonance interaction parameters of the main,  $^{12}\text{C}_2\text{H}_4$ , species (with the exception of the main Coriolis parameters) were used as the initial values of corresponding parameters for  $^{13}\text{C}_2\text{H}_4$ .

The parameters  $C^1 (2A\zeta, 2B\zeta, 2C\zeta)$  strongly correlate with the rotational parameters of corresponding interacting vibrational states. For that reason we preferred not to vary them in the further weighted fit procedure the results of which are presented in Tables 9 and 10. Values in parentheses in these tables are  $1\sigma$  statistical confidence intervals. Parameters presented without confidence intervals have been constrained to their initial values (see above). One can see that the values of parameters in columns 3, 5, 7, and 9 of Table 9 correspond more than satisfactorily to the values of parameters of the ground vibrational state (the latter are re-presented in column 2 of Table 9 from Table 6). For comparison, columns 4, 6, 8, and 10 of Table 9 present values of corresponding parameters of the  $^{12}\text{C}_2\text{H}_4$  species from Ref. [27]. One can see an expected good correspondence between both sets of parameters. It can be interesting to compare the values of the band centers obtained from analysis of experimental data and ones derived from recent *ab initio* calculations, Ref. [54]. The *ab initio* values of the band centers are:  $\nu_4 = 1025.14\text{ cm}^{-1}$ ,  $\nu_7 = 944.50\text{ cm}^{-1}$ ,  $\nu_{10} = 821.22\text{ cm}^{-1}$ ,  $\nu_{12} = 1434.90\text{ cm}^{-1}$ . One can see satisfactory agreement of *ab initio* results with the experimental data from Table 9.

General vibration-rotation theory states that the diagonal block parameters can differ from corresponding parameters of the ground vibrational state not more than a few percent, see, e.g., Ref. [55]. Therefore, following the strategy of the recent paper, Ref. [27], we varied only band centers, rotational and the most important (quartic) centrifugal distortion parameters. If the value of a varied centrifugal distortion parameter was less or even comparable with its  $1\sigma$  statistical confidence interval, it was

**Table 7**

Small part of experimental ro-vibrational term values for the ( $v_7 = 1$ ), ( $v_{10} = 1$ ), and ( $v_{12} = 1$ ) vibrational state of the  $^{13}\text{C}_2\text{H}_4$  molecule (in  $\text{cm}^{-1}$ )<sup>a</sup>.

Band			$\nu_7$			$\nu_{10}$			$\nu_{12}$		
$J$	$K_a$	$K_c$	$E$	$\Delta$	$\delta$	$E$	$\Delta$	$\delta$	$E$	$\Delta$	$\delta$
1			2	3	4	2	3	4	2	3	4
7	0	7	991.97476	17	3				1484.98895	5	-2
7	1	7	994.42382	18	-1	875.01633	36	-1	1487.21451	4	-2
7	1	6	998.61899	10	3	879.01818	15	13	1491.80340	5	1
7	2	6	1009.05581	10	2	888.60416	16	4	1501.72265	1	-1
7	2	5	1009.55455	7	-2	889.09629	6	7	1502.33334	7	-1
7	3	5	1029.98200	8	0	907.96951	19	5	1522.13253	11	8
7	3	4	1029.99635	10	0	907.98428	21	7	1522.15239	2	3
7	4	4	1059.03659	6	0	934.87660	22	6	1550.43088	29	5
7	4	3	1059.03659	6	-16	934.87660	22	-10	1550.43088	29	-18
7	5	3	1096.37007	16	0	969.50479	12	2	1586.81882	4	3
7	5	2	1096.37007	16	0	969.50479	12	2	1586.81882	4	3
7	6	2	1141.95066	7	1	1011.85949	16	-4	1631.27970	8	0
7	6	1	1141.95066	7	1	1011.85949	16	-4	1631.27970	8	0
7	7	1	1195.74660	3	2	1061.94674	13	-5	1683.79481	10	4
7	7	0	1195.74660	3	2	1061.94674	13	-5	1683.79481	10	4
8	0	8	1005.57177	10	6				1498.58596	5	-6
8	1	8	1007.66557	7	1	888.18976	33	9	1500.45150	3	-1
8	1	7	1013.04575	10	-5	893.32128	19	-12	1506.33281	1	0
8	2	7	1022.92077	8	-3	902.37342	18	-17	1515.64512	3	0
8	2	6	1023.73824	5	-2	903.17949	13	6	1516.64212	2	8
8	3	6	1043.93422	10	1	921.82732	6	-4	1536.16388	6	4
8	3	5	1043.96566	7	-1	921.85974	8	4	1536.20737	17	-7
8	4	5	1072.97255	11	-9	948.72234	4	8	1564.44785	41	35
8	4	4	1072.97305	12	-6	948.72267	10	-9	1564.44785	41	-38
8	5	4	1110.29192	11	3	983.34117	12	-2	1600.82368	4	2
8	5	3	1110.29192	11	6	983.34117	12	-3	1600.82368	4	1
8	6	3	1155.85897	8	-1	1025.69038	13	7	1645.27736	8	2
8	6	2	1155.85897	8	-1	1025.69038	13	7	1645.27736	8	2
8	7	2	1209.63631	8	6	1075.77333	9	-4	1697.78722	4	2
8	7	1	1209.63631	8	6	1075.77333	9	-4	1697.78722	4	2
8	8	1	1271.57840	7	0	1133.59637	9	7	1758.33329	9	0
8	8	0	1271.57840	7	0	1133.59637	9	7	1758.33329	9	0
9	0	9	1020.78715	22	3				1513.78852	3	-1
9	1	9	1022.54174	15	0	902.98943	33	18	1515.31833	3	-1
9	1	8	1029.24303	17	-3	909.37987	5	-17	1522.63691	6	0
9	2	8	1038.50118	18	-2	917.84664	10	-3	1531.28605	8	-5
9	2	7	1039.75725	7	-5	919.08362	18	19	1532.81022	9	-2
9	3	7	1059.63720	11	7	937.42380	5	-3	1551.95655	8	3
9	3	6	1059.69974	11	-2	937.48823	9	5	1552.04318	48	0
9	4	6	1088.65695	10	7	964.30470	15	3	1580.22470	62	99
9	4	5	1088.65820	9	12	964.30587	-12	1580.22470	62	-93	
9	5	5	1125.95790	10	-6	998.91079	23	0	1616.58370	3	3
9	5	4	1125.95790	10	6	998.91079	23	-2	1616.58370	3	1
9	6	4	1171.50868	6	6	1041.25226	13	8	1661.02755	2	-1
9	6	3	1171.50868	6	6	1041.25226	13	7	1661.02755	2	-1
9	7	3	1225.26469	9	-5	1091.32967	4	-3	1713.53056	5	1
9	7	2	1225.26469	9	-5	1091.32967	4	-3	1713.53056	5	1
9	8	2	1287.15060	10	4	1149.14797	2	1	1774.07114	4	1
9	8	1	1287.15060	10	4	1149.14797	2	1	1774.07114	4	1
9	9	1	1357.59708	15	0	1214.71151	10	1	1842.62768	2	-3
9	9	0	1357.59708	15	0	1214.71151	10	1	1842.62768	2	-3

<sup>a</sup>  $\Delta$  is the experimental uncertainty in the upper energy value in units of  $10^{-5} \text{ cm}^{-1}$  ( $\Delta$  is absent when the upper energy value was determined from a single transition);  $\delta$  is the difference  $E^{\text{exp.}} - E^{\text{calc.}}$  also in units of  $10^{-5} \text{ cm}^{-1}$ .

constrained to its initial value. To achieve a satisfactory correspondence between theoretical and experimental results, the number of varied resonance interaction parameters is larger than usually used in analogous fits.

One remark should be made here. At least three of the four considered vibrational states are located very close to each other, and even a minor change of their relative location can change strongly both the strength and the

quality of interactions. In our case, as is seen from Table 3, the centers of two bands ( $\nu_7$  and  $\nu_{12}$ ) are moved by  $5-6 \text{ cm}^{-1}$ , while the centers of the other bands ( $\nu_4$  and  $\nu_{10}$ ) are practically unchanged. This leads to a change of relative positions of vibrational energy levels, and, as a consequence, to a change of both the quantitative and qualitative picture of higher order resonance interaction parameters. For that reason, the main resonance interaction

**Table 8**Experimental ro-vibrational term values of the ( $v_4 = 1, A_u$ ) vibrational state of the  $^{13}\text{C}_2\text{H}_4$  molecule (in  $\text{cm}^{-1}$ ).<sup>a</sup>

$J$	$K_a$	$K_c$	$E$	$\Delta$	$\delta$	$J$	$K_a$	$K_c$	$E$	$\Delta$	$\delta$	$J$	$K_a$	$K_c$	$E$	$\Delta$	$\delta$
1			2	3	4	1			2	3	4	1			2	3	4
6	6	0	1202.80570	19	22	13	9	5	1500.33343	3	-7	17	10	8	1682.84241	17	1
6	6	1	1202.80570	19	22	13	9	4	1500.33343	3	-7	17	10	7	1682.84241	17	1
7	6	2	1215.12781	43	14	13	10	4	1574.20784	22	-23	18	6	13	1467.18047	30	26
7	6	1	1215.12781	43	14	13	10	3	1574.20784	22	-23	18	6	12	1467.18047	30	-65
7	7	1	1265.64914	-23	14	6	9	9	1350.76897	9	4	18	7	12	1517.98010	22	-18
7	7	0	1265.64914	-23	14	6	8	8	1350.76897	9	-1	18	7	11	1517.98010	22	-20
8	7	1	1279.77591	30	14	7	8	1401.54319	10	2	18	8	11	1572.49154	5	0	
8	7	2	1279.77591	30	14	7	7	1401.54319	10	2	18	8	10	1572.49154	5	0	
9	6	4	1245.05881	45	-20	14	8	7	1463.12883	9	1	18	9	10	1640.35580	10	4
9	6	3	1245.05881	45	-20	14	8	6	1463.12883	9	1	18	9	9	1640.35580	10	4
9	7	3	1295.66466	10	5	14	9	6	1524.83638	11	9	18	10	9	1714.38331	18	-1
9	7	2	1295.66466	10	5	14	9	5	1524.83638	11	9	18	10	8	1714.38331	18	-1
9	8	2	1353.60353	6	0	14	10	5	1598.73735	-11	19	6	14	1500.71863	10	3	
9	8	1	1353.60353	6	0	14	10	4	1598.73735	-11	19	6	14	1500.72063		10	
10	6	5	1262.66971	6	2	15	6	10	1377.21392	27	-4	19	7	13	1551.50254	28	-2
10	6	4	1262.66971	6	2	15	6	9	1377.21392	27	7	19	7	12	1551.50254	28	-6
10	7	4	1313.31603	8	5	15	7	9	1428.00642	11	3	19	8	12	1605.53381	15	3
10	7	3	1313.31603	8	5	15	7	8	1428.00642	11	3	19	8	11	1605.53381	15	3
10	8	3	1370.95279	2	0	15	8	8	1483.83491	3	-1	19	9	11	1673.61290	21	2
10	8	2	1370.95279	2	0	15	8	7	1483.83491	3	-1	19	9	10	1673.61290	21	2
11	7	5	1332.72950	41	1	15	9	7	1551.08987	31	1	19	10	10	1747.67753	16	11
11	7	4	1332.72950	41	1	15	9	6	1551.08987	31	1	19	10	9	1747.67753	16	11
11	8	4	1390.04354	13	-2	15	10	6	1625.01960	24	27	20	7	14	1586.79208	8	-2
11	8	3	1390.04354	13	-2	15	10	5	1625.01960	24	27	20	7	13	1586.79208	8	-12
11	9	3	1456.58012	9	12	16	6	11	1405.42978	35	-18	20	8	13	1640.32142	13	-5
11	9	2	1456.58012	9	12	16	6	10	1405.42978	35	25	20	8	12	1640.32142	13	-5
11	10	2	1530.40636	-65	16	7	10	1456.23312	4	-2	20	9	12	1708.62089	7	4	
11	10	1	1530.40636	-65	16	7	9	1456.23312	4	-2	20	9	11	1708.62089	7	4	
12	6	7	1303.18582	15	1	16	8	9	1511.64238	21	0	20	10	11	1782.72505		27
12	6	6	1303.18582	15	1	16	8	8	1511.64238	21	0	20	10	10	1782.72505		27
12	7	6	1353.90499	7	-9	16	9	8	1579.09415	9	3	21	6	16	1573.13098		-20
12	7	5	1353.90499	7	-9	16	9	7	1579.09415	9	4	21	6	15	1573.13742	18	-10
12	8	5	1410.87658	8	1	16	10	7	1653.05449	-13	21	7	15	1623.85020		2	
12	8	4	1410.87658	8	1	16	10	6	1653.05449	-2	21	7	14	1623.85020		-16	
12	9	4	1477.58169	26	2	17	6	12	1435.41812	33	29	21	8	14	1676.85482	11	3
12	9	3	1477.58169	26	2	17	6	11	1435.41812	33	-22	21	8	13	1676.85482	11	3
13	6	8	1326.09347	13	9	17	7	11	1486.22425	24	10	21	9	13	1745.37958	34	-5
13	6	7	1326.09347	13	7	17	7	10	1486.22425	24	10	21	9	12	1745.37958	34	-5
13	7	7	1376.84289	15	1	17	8	10	1541.19445	18	-4	21	10	12	1819.52537	21	-14
13	7	6	1376.84289	15	1	17	8	9	1541.19445	18	-4	21	10	11	1819.52537	21	-14
13	8	6	1433.45243	5	-2	17	9	9	1608.84950	17	-5	22	6	17	1612.00941		-7
13	8	5	1433.45243	5	-2	17	9	8	1608.84950	17	-5	22	6	16	1612.02058		13
22	7	16	1662.67830	24	16	26	10	17	2029.83278	4	8	31	10	22	2283.98205	12	-8
22	7	15	1662.67830	24	-19	26	10	16	2029.83278	4	8	31	10	21	2283.98205	12	-8
22	8	15	1715.13389	38	4	27	7	21	1883.42160	-16	32	0	32	1888.16205	10	-8	
22	8	14	1715.13389	38	4	27	7	20	1883.42776	2	32	9	24	2265.19927	22	-12	
22	9	14	1783.88908	17	0	27	8	20	1932.71677	19	-18	32	9	23	2265.19933	22	-24

22	9	13	1783.88908	17	0	27	8	19	1932.71677	19	– 28	32	10	23	2340.07239	– 17
22	10	13	1858.07952	20	– 19	27	9	19	2002.68844	11	– 1	32	10	22	2340.07239	– 17
22	10	12	1858.07952	20	– 19	27	9	18	2002.68844	11	– 2	33	9	25	2322.93904	13
23	6	18	1652.67222	29	28	27	10	18	2077.15523	21	1	33	9	24	2322.93904	7
23	6	17	1652.69038	29	2	27	10	17	2077.15523	21	1	33	10	24	2397.91608	2
23	8	16	1755.15886	19	7	28	7	22	1932.90371	1	0	33	10	23	2397.91608	3
23	8	15	1755.15886	19	7	28	8	21	1981.47044	7	8	34	8	27	2310.60105	15
23	9	15	1824.14902	14	– 3	28	8	20	1981.47044	7	– 9	34	9	26	2382.42187	11
23	9	14	1824.14902	14	– 3	28	9	20	2051.69623	10	8	34	9	25	2382.42187	21
23	10	14	1898.38750		3	28	9	19	2051.69623	10	7	34	10	25	2457.51245	2
23	10	13	1898.38750		3	28	10	19	2126.23150	29	1	34	10	24	2457.51245	4
24	8	17	1796.92961	8	– 1	28	10	18	2126.23150	29	1	35	0	35	2069.17720	34
24	8	16	1796.92961	8	– 2	29	6	23	1934.48551		8	35	8	28	2371.54432	21
24	9	16	1866.15920	14	– 10	29	7	22	1984.18362		– 18	35	8	27	2371.54801	16
24	9	15	1866.15920	14	– 10	29	8	21	2031.96878	23	– 10	35	9	27	2443.64693	25
24	10	15	1940.44863	17	– 20	29	9	21	2102.45193	10	5	35	9	26	2443.64693	28
24	10	14	1940.44863	17	– 20	29	9	20	2102.45193	10	4	35	10	26	2518.86106	20
25	6	19	1739.40610	3	– 4	29	10	20	2177.06129	9	– 15	35	10	25	2518.86106	23
25	8	18	1840.44638	18	5	29	10	19	2177.06129	9	– 15	36	0	36	2130.19720	2
25	8	17	1840.44638	18	1	30	0	30	1786.35070	23	1	36	8	29	2434.22109	18
25	9	17	1909.91963	16	2	30	6	24	1987.80716	18	8	36	8	28	2434.22580	12
25	9	16	1909.91963	16	2	30	7	24	2037.21630	34	5	36	9	28	2506.61246	13
25	10	16	1984.26393	10	8	30	7	23	2037.24144		– 5	36	9	27	2506.61311	6
25	10	15	1984.26393	10	8	30	8	21	2084.21128	46	21	37	8	30	2498.62766	10
26	6	20	1785.46107	9	9	30	8	20	2084.21128	46	– 22	37	8	29	2498.63345	28
26	8	19	1885.70887	6	3	30	9	22	2154.95509	29	19	37	9	29	2571.31782	58
26	8	18	1885.70887	6	– 3	30	9	21	2154.95509	29	15	37	9	28	2571.31782	72
26	9	18	1955.42941	17	0	31	9	23	2209.20425		– 12	38	0	38	2256.99309	10
26	9	17	1955.42941	17	0	31	9	22	2209.20425		– 19	38	8	31	2564.75900	19

<sup>a</sup>  $\Delta$  is the experimental uncertainty in the upper energy value in units of  $10^{-5} \text{ cm}^{-1}$  ( $\Delta$  is absent when the upper energy value was determined from a single transition);  $\delta$  is the difference  $E^{\text{exp.}} - E^{\text{calc.}}$  also in units of  $10^{-5} \text{ cm}^{-1}$ .

**Table 9**

Spectroscopic parameters of the ( $v_4 = 1$ ), ( $v_7 = 1$ ), ( $v_{10} = 1$ ), and ( $v_{12} = 1$ ) vibrational states of the  $^{13}\text{C}_2\text{H}_4$  molecule (in  $\text{cm}^{-1}$ ).<sup>a</sup>

Parameter	Gr. st.	$^{13}\text{C}_2\text{H}_4$ , tw	( $v_4 = 1$ ), $^{13}\text{C}_2\text{H}_4$ , tw	( $v_4 = 1$ ) $^{12}\text{C}_2\text{H}_4$ , [27]	( $v_7 = 1$ ), $^{13}\text{C}_2\text{H}_4$ , tw	( $v_7 = 1$ ) $^{12}\text{C}_2\text{H}_4$ , [27]	( $v_{10} = 1$ ), $^{13}\text{C}_2\text{H}_4$ , tw	( $v_{10} = 1$ ) $^{12}\text{C}_2\text{H}_4$ , [27]	( $v_{12} = 1$ ), $^{13}\text{C}_2\text{H}_4$ , tw	( $v_{12} = 1$ ) $^{12}\text{C}_2\text{H}_4$ , [27]
1	2	3	4	5	6	7	8	9	10	
$E$		1025.804276 (85)	1025.5897759	943.762440 (12)	948.77090402	824.915109 (18)	825.9267614	1436.651008 (11)	1442.4424016	
$A$	4.864792048	4.8462095 (23)	4.8462200	4.87097955 (50)	4.86898055	4.87165258 (88)	4.8734698	4.85182068 (48)	4.85206671	
$B$	0.9506945106	0.9485494 (15)	0.99881574	0.94848783 (24)	0.99887651	0.94980454 (41)	1.000116099	0.95340739 (69)	1.00392569	
$C$	0.7932735014	0.7931810 (19)	0.82807345	0.79442288 (44)	0.82934142	0.79169067 (79)	0.826394802	0.79164114 (75)	0.82633727	
$\Delta_K \times 10^4$	0.8701743	0.8701743	0.86470155	0.88832 (19)	0.86470155	0.8701743	0.8861073	0.88066 (48)	0.866649	
$\Delta_{JK} \times 10^4$	0.09815297	0.09815297	0.0987461	0.0906 (11)	0.1028003	0.11076 (83)	0.102336194	0.09790 (16)	0.1116283	
$\Delta_J \times 10^4$	0.013386718	0.013439 (13)	0.014701077	0.013465 (14)	0.01475178	0.013301 (11)	0.014701077	0.013425 (14)	0.01474409	
$\delta_K \times 10^4$	0.0953733	0.0953733	0.1017914	0.0953733	0.09751825	0.0953733	1.036307	0.09182 (23)	0.1048415	
$\delta_j \times 10^4$	0.002452716	0.002452716	0.0028179017	0.0024404 (71)	0.00280751	0.0023983 (68)	0.0028179017	0.0025053 (68)	0.00289684	
$H_K \times 10^8$	0.628947	0.628947	0.621279	0.6422 (17)	0.64669	0.628947	0.621279	0.628947	0.621279	
$H_{KJ} \times 10^8$	– 0.0431669	– 0.0431669	– 0.041497	– 0.0431669	– 0.041497	– 0.0431669	– 0.041497	– 0.0431669	– 0.041497	
$H_{JK} \times 10^8$	0.0166920	0.0166920	0.018693	0.01858 (13)	0.014952	0.0166920	0.018693	0.0166920	0.018693	
$H_J \times 10^8$	0.00029659	0.00029659	0.00023588	0.00029659	0.0002164	0.00029659	0.00023588	0.00029659	0.00023588	
$h_K \times 10^8$	0.34059	0.34059	0.34059	0.34059	0.34059	0.34059	0.34059	0.34059	0.34059	
$h_{JK} \times 10^8$	0.0103566	0.0103566	0.0103566	0.0103566	0.0103566	0.0103566	0.0103566	0.0103566	0.0103566	
$h_j \times 10^8$	0.000125178	0.000125178	0.000125178	0.000125178	0.000125178	0.000125178	0.000125178	0.000125178	0.000125178	
$L_K \times 10^{12}$	– 0.4467	– 0.4467	– 0.4467	– 0.4467	– 0.4467	– 0.4467	– 0.4467	– 0.4467	– 0.4467	
$L_{JK} \times 10^{12}$	– 0.004492	– 0.004492	– 0.004492	– 0.004492	– 0.004492	– 0.004492	– 0.004492	– 0.004492	– 0.004492	
$L_j \times 10^{12}$	– 0.0000172	– 0.0000172	– 0.0000172	– 0.0000172	– 0.0000172	– 0.0000172	– 0.0000172	– 0.0000172	– 0.0000172	

<sup>a</sup> Values in parentheses are  $1\sigma$  standard errors.

**Table 10**Coriolis interaction parameters for the ( $v_4 = 1, A_u$ ), ( $v_7 = 1, B_{1u}$ ), ( $v_{10} = 1, B_{2u}$ ), and ( $v_{12} = 1, B_{3u}$ ) vibrational states of the  $^{13}\text{C}_2\text{H}_4$  molecule (in  $\text{cm}^{-1}$ ).<sup>a</sup>

Parameter	Value	Parameter	Value	Parameter	Value
$^{4.7}C_K^1 \times 10^4$	0.538(22)	$^{4.7}C_J^1 \times 10^5$	0.157(16)	$^{4.7}C_{KK}^1 \times 10^6$	– 0.1338(27)
$^{4.7}C^2 \times 10^2$	0.5360(16)	$^{4.7}C_K^2 \times 10^6$	0.501(41)	$^{4.7}C_J^2 \times 10^6$	– 0.199(16)
$^{4.7}C_{JJ}^2 \times 10^{10}$	0.1073(47)				
$(2B\zeta^x)^{4.10}$	– 1.68	$^{4.10}C_K^1 \times 10^3$	0.15012(87)	$^{4.10}C_J^1 \times 10^5$	0.750(13)
$^{4.10}C_{KK}^1 \times 10^7$	0.782(24)	$^{4.10}C^2 \times 10^2$	– 0.4964(30)	$^{4.10}C_K^2 \times 10^6$	0.863(61)
$(2A\zeta^z)^{4.12}$	– 5.48	$^{4.12}C_K^1 \times 10^3$	0.17585(27)	$^{4.12}C_J^1 \times 10^4$	0.2645(53)
$^{4.12}C_{KJ}^1 \times 10^7$	0.1216(20)	$^{4.12}C^2 \times 10^2$	0.1036(30)		
$(2A\zeta^z)^{7.10}$	– 4.40	$^{7.10}C_K^1 \times 10^4$	0.8272(53)	$^{7.10}C_J^1 \times 10^4$	0.2272(84)
$^{7.10}C_{KJ}^1 \times 10^7$	– 0.1088(16)	$^{7.10}C^2 \times 10^3$	– 0.2804(16)		
$(2B\zeta^y)^{7.12}$	– 1.25	$^{7.12}C_K^1 \times 10^3$	0.1342(16)	$^{7.12}C_J^1 \times 10^4$	0.1197(57)
$^{7.12}C^2 \times 10$	– 0.12399(57)				
$(2C\zeta^y)^{10.12}$	0.13	$^{10.12}C_J^1 \times 10^4$	– 0.1312(55)	$^{10.12}C_J^2 \times 10^3$	– 0.10577

<sup>a</sup> Values in parentheses are  $1\sigma$  standard errors.

parameters in our fit, as was mentioned above, were fixed to the theoretically predicted values, and higher order interaction parameters were varied irrespective of the values of corresponding higher order parameters in the  $^{12}\text{C}_2\text{H}_4$  species, Ref. [27].

A set of 55 parameters (31 parameters of four diagonal blocks and 24 resonance interaction parameters) was obtained from the fit. They reproduce values of the 2934 “experimental” ro-vibrational energies of the states ( $v_4 = 1$ ), ( $v_7 = 1$ ), ( $v_{10} = 1$ ), and ( $v_{12} = 1$ ) (obtained from more than 9500 transitions of the bands  $\nu_4$ ,  $\nu_7$ ,  $\nu_{10}$ , and  $\nu_{12}$ ) with  $d_{\text{rms}} = 0.00014 \text{ cm}^{-1}$ . To illustrate the quality of the fit, column 4 of Tables 7 and 8 presents the values  $\delta$  (in  $10^{-5} \text{ cm}^{-1}$ ) which are the differences between the “experimental” values of upper ro-vibrational energies and corresponding values calculated with the parameters obtained in the present study. One can see more than satisfactory correspondence between “experimental” and calculated values.

## 8. Conclusion

We re-analyzed the high resolution ro-vibrational structure of the  $\nu_{12}$  band and, for the first time made an analysis of the bands  $\nu_4$ ,  $\nu_7$ , and  $\nu_{10}$  of the  $^{13}\text{C}_2\text{H}_4$  molecule. The ground vibrational state was re-analyzed on the basis of new experimental data. The improved set of ground state parameters was obtained, and used for determination of upper ro-vibrational energy values. The latter were fitted in a Hamiltonian model which takes into account resonance interactions between all four studied vibrational states, ( $v_4 = 1$ ), ( $v_7 = 1$ ), ( $v_{10} = 1$ ), and ( $v_{12} = 1$ ). The energy values obtained from the fit set of 55 parameters reproduce the initial FTIR data within accuracies close to experimental uncertainties.

## Acknowledgments

The work was supported by the project Leading Russian Research Universities (Grant FTI-120 of the Tomsk Polytechnic University). Part of the work was supported by the

Foundation of the President of the Russian Federation (Grant MK-4872.2014.2) and by the Deutsche Forschungsgemeinschaft (Grants BA 2176/3-2 and BA 2176/4-1).

## Appendix A. Supplementary data

Supplementary data associated with this paper can be found in the online version at <http://dx.doi.org/10.1016/j.jqsrt.2014.09.024>.

## References

- [1] Abele FB, Heggetad HE. Ethylene: an urban air pollutant. *J Air Pollut Control Assoc* 1973;23:517–21.
- [2] Betz L. Ethylene in IRC10216. *Astrophys J* 1981;244:L103–5.
- [3] Cernicharo J, Heras AM, Pardo JR, Tielens AGGM, Guelin M, Dartois E, et al. Methylpolyyne and small hydrocarbons in CRL 618. *Astrophys J* 2001;546:L127–30.
- [4] Kostiuk T, Romani P, Espenak F, Livengood TA, Goldstein JJ. Temperature and abundances in the jovian auroral stratosphere 2. Ethylene as a probe of the microbar region. *J Geophys Res* 1993;98:18823–30.
- [5] Griffith CA, Bézard B, Greathouse TK, Kelly DM, Lacy JH, Noll KS. Thermal infrared imaging spectroscopy of Shoemaker-Levy 9 impact sites: spatial and vertical distributions of  $\text{NH}_3$ ,  $\text{C}_2\text{H}_4$ , and  $10 \mu\text{m}$  dust emission. *Icarus* 1997;128:275–93.
- [6] Bézard B, Moses JL, Lacy J, Greathouse T, Richter M, Griffith C. Detection of ethylene ( $\text{C}_2\text{H}_4$ ) on Jupiter and Saturn in non-auroral regions. *Bull Am Astron Soc* 2001;33:1079.
- [7] Schulz B, Encrenaz T, Bézard B, Romani P, Lellouch E, Atreya SK. Detection of  $\text{C}_2\text{H}_4$  in Neptune from ISO/PHTS observations. *Astron Astrophys* 1999;350:L13–7.
- [8] Saslaw WC, Wildey RL. On the chemistry of Jupiter's upper atmosphere. *Icarus* 1967;7:85–93.
- [9] Coustenis A, Achterberg RK, Conrath BJ, Jennings DE, Marten A, Gautier D, et al. The composition of Titan's stratosphere from Cassini CIRS midinfrared spectra. *Icarus* 2007;189:35–62.
- [10] Kunde VG, Aikin AC, Hanel RA, Jennings DE, Maguire WC, Samuelson RE.  $\text{C}_4\text{H}_2$ ,  $\text{HC}_3\text{N}$  and  $\text{C}_2\text{N}_2$  in Titan's atmosphere. *Nature* 1981;292:686–8.
- [11] Bar-Nun A, Podolak M. The photochemistry of hydrocarbons in Titan's atmosphere. *Icarus* 1979;38:115–22.
- [12] Coustenis A, Salama A, Schulz B, Ott S, Lellouch E, Encrenaz Th, et al. Titan's atmosphere from ISO mid-infrared spectroscopy. *Icarus* 2003;161:383–403.
- [13] Vervack Jr. RJ, Sandel BR, Strobel DF. New perspectives on Titan's upper atmosphere from a reanalysis of the Voyager 1 UVS solar occultations. *Icarus* 2004;170:91–112.

- [14] Rusinek E, Fichoux H, Khelkhal M, Herlemont F, Legrand J, Fayt A. Subdoppler study of the  $\nu_7$  band of  $C_2H_4$  with a  $CO_2$  laser sideband spectrometer. *J Mol Spectrosc* 1998;189:64–73.
- [15] Tan TL, Lau SY, Ong PP, Goh KL, Teo HH. High-resolution fourier transform infrared spectrum of the  $\nu_{12}$  fundamental band of ethylene ( $C_2H_4$ ). *J Mol Spectrosc* 2000;203:310–3.
- [16] Duncan JL, Robertson GE. Vibrational anharmonicity in ethylenic compounds. *J Mol Spectrosc* 1991;145:251–61.
- [17] Martin JML, Lee TJ, Taylor PR, François JP. The anharmonic force field of ethelene,  $C_2H_4$ , by means of accurate *ab initio* calculations. *J Chem Phys* 1995;103:2589–602.
- [18] Rotger M, Boudon V, Vander Auwera J. Line positions and intensities in the  $\nu_{12}$  band of ethylene near  $1450\text{ cm}^{-1}$ : an experimental and theoretical approach. *J Quant Spectrosc Radiat Transf* 2008;109:952–62.
- [19] Gonzalez LMA, Boudon V, Loete M, Rotger M, Bourgeois MT, Didricle K, et al. High-resolution spectroscopy and preliminary global analysis of C-H stretching vibrations of  $C_2H_4$  in the 3000 and  $6000\text{ cm}^{-1}$  regions. *J Quant Spectrosc Radiat Transf* 2010;111:2265–78.
- [20] Vander Auwera J, Fayt A, Tudorie M, Rotger M, Boudon V, Franco B, Mahieu E. Self-broadening coefficients and improved line intensities for the  $\nu_7$  band of ethylene near  $10.5\text{ }\mu\text{m}$ , and impact on ethylene retrievals from Jungfraujoch solar spectra. *J Quant Spectrosc Radiat Transf* 2014;148:177–85.
- [21] Rothman LS, Gordon IE, Babikov Y, Barbe A, Chris Benner D, Bernath PF, et al. The HITRAN2012 molecular spectroscopic database. *J Quant Spectrosc Radiat Transf* 2013;130:4–50.
- [22] Ba YA, Wenger C, Surleau R, Boudon V, Rotger M, Daumont L, et al. MeCaSda and ECaSda: methane and ethene calculated spectroscopic databases for the virtual atomic and molecular data center. *J Quant Spectrosc Radiat Transf* 2013;130:62–8.
- [23] Tan TL, Goh KL, Ong PP, Teo HH. Analysis of the  $\nu_{12}$  band of ethylene- $^{13}C_2$  by high-resolution FTIR spectroscopy. *J Mol Spectrosc* 2001;207:189–92.
- [24] Tan TL, Kang LL, Goh KL, Teo HH. Analysis of the  $\nu_{11}$  band of ethylene- $^{13}C_2$  by high-resolution FTIR spectroscopy. *Chem Phys Lett* 2004;393:343–6.
- [25] Ulenikov ON, Onopenko GA, Bekhtereva ES, Petrova TM, Solodov AM, Solodov AA. High resolution study of the  $\nu_5 + \nu_{12}$  band of  $C_2H_4$ . *Mol Phys* 2010;108:637–47.
- [26] Tan TL, Gabona MG, Lebron GB. The  $\nu_{12}$  band of  $C_2D_4$ . *J Mol Spectrosc* 2011;266:113–5.
- [27] Ulenikov ON, Gromova OV, Aslapovskaya YuS, Horneman VM. High resolution spectroscopic study of  $C_2H_4$ : re-analysis of the ground state and  $\nu_4$ ,  $\nu_7$ ,  $\nu_{10}$ , and  $\nu_{12}$  vibrational bands. *J Quant Spectrosc Radiat Transf* 2013;118:14–25.
- [28] Gabona MG, Tan TL. Improved ground state and  $\nu_{12}=1$  state rovibrational constants for ethylene- $^{13}C_2$  ( $^{13}C_2H_4$ ). *J Mol Spectrosc* 2014;299:35–7.
- [29] Ulenikov ON, Gromova OV, Bekhtereva ES, Onopenko GA, Aslapovskaya YuS, Gericke KH. High resolution FTIR study of the  $\nu_7 + \nu_{10} - \nu_{10}$  and  $\nu_{10} + \nu_{12} - \nu_{10}$  “hot” bands of  $C_2H_4$ . *J Quant Spectrosc Radiat Transfer* 2014;149:318–33.
- [30] Duncan JL, McKean DC, Mallinson PD. Infrared cristal spectra of  $C_2H_4$ ,  $C_2D_4$ , and as- $C_2D_2$  and the general harmonic force field of ethylene. *J Mol Spectrosc* 1973;45:221–46.
- [31] Makushkin YuS, Ulenikov ON. Isotopic relationships for polyatomic molecules. *Opt Spectrosc* 1975;39:629–36.
- [32] Bykov AD, Makushkin YuS, Ulenikov ON. On isotope effects in polyatomic molecules: some comments on the method. *J Mol Spectrosc* 1981;85:462–79.
- [33] Bykov AD, Makushkin YuS, Ulenikov ON. On the displacements of centers of vibration-rotation bands under isotope substitution in polyatomic molecules. *J Mol Spectrosc* 1982;93:46–54.
- [34] Bykov AD, Makushkin YuS, Ulenikov ON. On the displacements of centers of vibration-rotation lines under isotope substitution in polyatomic molecules. *Mol Phys* 1984;51:907–18.
- [35] Maki AG, Wells JS. Wavenumber calibration tables from heterodyne frequency measurements (version 1.3). Gaithersburg, MD: National Institute of Standards and Technology; 1998.
- [36] Flaud JM, Camy-Peyret C. The interacting states (020), (100), and (001) of  $H_2^{18}O$ . *J Mol Spectrosc* 1974;51:142–50.
- [37] Antipov AB, Bykov AD, Kapitanov VA, Lopasov, Makushkin Yus, Tolmachev VI, et al. Water-vapor absorption spectrum in the  $0.59 - \mu\text{m}$  region. *J Mol Spectrosc* 1981;89:449–59.
- [38] Ulenikov ON, Tolchenov RN, Koivusaari M, Alanko S, Anttila R. High-resolution Fourier transform spectra of  $CH_2D_2$ : pentade of the lowest interacting vibrational bands  $\nu_4(A_1)$ ,  $\nu_7(B_1)$ ,  $\nu_9(B_2)$ ,  $\nu_5(A_2)$ , and  $\nu_3(A_1)$ . *J Mol Spectrosc* 1994;167:109–30.
- [39] Makushkin YuS, Tyuterev VG. Methods of perturbations and effective Hamiltonians in molecular spectroscopy. Novosibirsk: Nauka; 1984.
- [40] Ulenikov ON, Onopenko GA, Lin H, Zhang JH, Zhou ZY, Zhu QS, Tolchenov RN. Joint rotational analysis of 24 bands of the  $H_2Se$  molecule. *J Mol Spectrosc* 1998;189:29–39.
- [41] Wang XH, Ulenikov ON, Onopenko GA, Bekhtereva ES, et al. High-resolution study of the first hexad of  $D_2O$ . *J Mol Spectrosc* 2000;200:25–33.
- [42] He SG, Ulenikov ON, Onopenko GA, Bekhtereva ES, Wang XH, Hu SM, et al. High-resolution Fourier transform spectrum of the  $D_2O$  molecule in the region of the second triad of interacting vibrational states. *J Mol Spectrosc* 2000;200:34–9.
- [43] Ulenikov ON, He SG, Onopenko GA, Bekhtereva ES, Wang XH, Hu SM, et al. High-resolution study of the ( $\nu_1 + \frac{1}{2}\nu_2 + \nu_3 = 3$ ) polyad of strongly interacting vibrational bands of  $D_2O$ . *J Mol Spectrosc* 2000;204:216–25.
- [44] Liu AW, Ulenikov ON, Onopenko GA, Gromova OV, Bekhtereva ES, Wan L, et al. Global fit of the high resolution infrared spectrum of  $D_2S$ . *J Mol Spectrosc* 2006;238:23–40.
- [45] Ulenikov ON, Bekhtereva ES, Grebneva SV, Hollenstein H, Quack M. High-resolution rovibrational analysis of vibrational states of  $A_2$  symmetry of the dideuterated methane  $CH_2D_2$ : the levels  $\nu_5$  and  $\nu_7 + \nu_9$ . *Mol Phys* 2006;104:3371–86.
- [46] Lafferty WJ, Flaud JM, Sams RL, Ngom EHA. High resolution analysis of the rotational levels of the (000), (010), (100), (001), (020), (110) and (011) vibrational states of  $^{34}S^{16}O_2$ . *J Mol Spectrosc* 2008;252:72–6.
- [47] Ulenikov ON, Bekhtereva ES, Albert S, Bauerecker S, Hollenstein H, Quack M. High-resolution near infrared spectroscopy and vibrational dynamics of dideuteromethane ( $CH_2D_2$ ). *J Phys Chem A* 2009;113:2218–31.
- [48] Ulenikov ON, Bekhtereva ES, Alanko S, Horneman FM, Gromova OV, Leroy C. On the high resolution spectroscopy and intramolecular potential function of  $SO_2$ . *J Mol Spectrosc* 2009;257:137–56.
- [49] Watson JKG. Determination of centrifugal distortion coefficients of asymmetric-top molecules. *J Chem Phys* 1967;46:1935–49.
- [50] Ulenikov ON. On the determination of the reduced rotational operator for polyatomic molecules. *J Mol Spectrosc* 1986;119:144–52.
- [51] Ulenikov ON, Malikova AB, Koivusaari M, Alanko S, Anttila R. High resolution vibrational-rotational spectrum of  $H_2S$  in the region of the  $\nu_2$  fundamental band. *J Mol Spectrosc* 1996;176:229–35.
- [52] Ulenikov ON, Bekhtereva ES, Grebneva SV, Hollenstein H, Quack M. High resolution Fourier transform spectroscopy of  $CH_2D_2$  in the region  $2350 - 2650\text{ cm}^{-1}$ : the bands  $\nu_5 + \nu_7$ ,  $2\nu_9$ ,  $\nu_3 + \nu_4$ ,  $\nu_3 + \nu_7$ , and  $\nu_5 + \nu_9$ . *Phys Chem Chem Phys* 2005;7:1142–50.
- [53] Makushkin YuS, Ulenikov ON. On the transformation of the complete electron-nuclear Hamiltonian of a polyatomic molecules to the intramolecular coordinates. *J Mol Spectrosc* 1977;68:1–20.
- [54] Delahaye T, Nikitin A, Rey M, Szalay PG, Tyuterev VG. A new accurate ground-state potential energy surface of ethylene and predictions for rotational and vibrational energy levels. *J Chem Phys* 2014;141:104301–16.
- [55] Papousek D, Aliev MR. Molecular vibrational-rotational spectra. Amsterdam: Elsevier; 1982.